Journal of Neuroscience Research 75:782–793 (2004)

Asymmetric Localization of LGN but Not AGS3, Two Homologs of *Drosophila* Pins, in Dividing Human Neural Progenitor Cells

Tannin J. Fuja,[1] Philip H. Schwartz,[1,2] Dan Darcy,[3] and Peter J. Bryant[1]*

[1]Developmental Biology Center, University of California, Irvine
[2]National Human Neural Stem Cell Resource and Stem Cell Research, Children's Hospital of Orange County Research Institute, Orange, California
[3]Biological Imaging Center, California Institute of Technology, Pasadena

Human neural progenitor cells (hNPCs) can be recovered from postmortem human brains and used to study the molecular basis of neurogenesis. Human NPCs are being used to investigate the molecular basis of cell fate determination during stem cell divisions, based on comparison with the *Drosophila* model system. *Drosophila* neuroblasts and sensory organ precursors undergo well-defined asymmetric cell divisions (ACD), under the control of a genetically defined set of apical and basal determinants that are localized tightly and dynamically during division. We show by indirect immunofluorescence, confocal microscopy, and time-lapse videomicroscopy that LGN and AGS3, two human homologs of the *Drosophila* ACD determinant Pins, have distinct patterns of localization in hNPCs. When cells are grown under conditions favoring proliferation, LGN is distributed asymmetrically in a cell cycle-dependent manner; it localizes to one side of the dividing cell and segregates into one of the daughter cells. When the cells are grown under conditions favoring differentiation, LGN accumulates in double foci similar to those containing the mitotic apparatus protein NuMA, and in a pattern shown previously for LGN and NuMA in differentiated cells. AGS3, a slightly more distant Pins homolog than LGN, does not show asymmetric localization in these cells. The progenitor cell marker nestin also localizes asymmetrically in colcemid-treated hNPCs and colocalizes with LGN. The results suggest that hNPCs undergo ACD and that similar molecular pathways may underlie these divisions in *Drosophila* and human cells. © 2004 Wiley-Liss, Inc.

Key words: asymmetric cell division, human neural progenitor cells, LGN, AGS3, NuMA, nestin, Pins

Asymmetric cell division (ACD) is a specialized type of mitotic cell division that results in unequal budding of a smaller cell from a larger progenitor or stem cell (Spana et al., 1995; Ceron et al., 2001; Knoblich, 2001; Schaefer and Knoblich, 2001). The progenitor cell can repetitively continue these divisions, whereas the smaller cell usually undergoes only a finite number of divisions before the progeny differentiate (Potten, 1997). Recent studies have raised new expectations for possible clinical uses of human embryonic or adult progenitor cells and focused attention on the need to understand the molecular controls of their development, division, and differentiation (Clarke et al., 2000; Temple, 2001; Jiang et al., 2002; Rathjen et al., 2002; Schwartz et al., 2002).

The genetic control of ACD in the *Drosophila* central and peripheral nervous system has been analyzed extensively; most essential genes are known, and the dynamic localization and functions of their protein products are understood well (Matsuzaki, 2000). Most *Drosophila* ACD determinants have clear human homologs, but the possible functions of these homologs in ACD have not been characterized. In *Drosophila*, one of the important apically localized ACD determinants is the Pins protein (Parmentier et al., 2000; Schaefer et al., 2000; Yu et al., 2000; Bellaiche et al., 2001). As a member of the apical complex with Bazooka/Par3, Par6, aPKC and Inscuteable, Pins is essential in the segregation of cell-fate determinants and the rotation of the mitotic spindle to properly orient the ACD. Pins binds directly to Inscuteable and is required for its apical localization (Bulgheresi et al., 2001). The mouse homolog of *Drosophila* Pins has been identified and is expressed in many mouse tissues but its expression is enriched in the ventricular zone of the developing CNS (Yu et al., 2003).

Contract grant sponsor: NCI; Contract grant number: CA91043; Contract grant sponsor: Salk Institute for Biological Studies; Contract grant sponsor: CHOC Foundation for Children; Contract grant sponsor: United Mitochondrial Disease Foundation; Contract grant sponsor: National Institute of Child Health and Human Development; Contract grant number: HD07029.

*Correspondence to: Peter J. Bryant, 4348 McGaugh Hall, University of California Irvine, Irvine, CA 92697. E-mail: pjbryant@uci.edu

Received 28 July 2003; Revised 17 October 2003; Accepted 21 October 2003

Supplementary Material for this article is available online at http://www.mrw.interscience.wiley.com/suppmat/0360-4012/suppmat/.

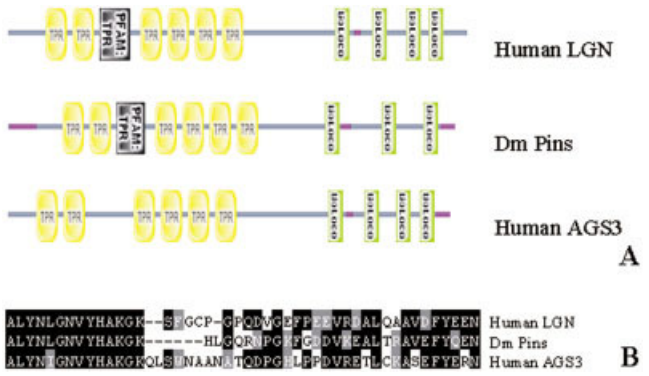

Fig. 1. The protein domain architecture of human LGN is closer than human AGS3 to *Drosophila* Pins. **A:** SMART protein domain architecture of *Drosophila* Pins and human LGN and AGS3. LGN and Pins have a PFAM (Protein Family) domain that is not found in AGS3. **B:** Megalign peptide sequence comparison of LGN, AGS3, and Pins at the regions of the PFAM domain detected by SMART.

Two human homologs of Pins have been identified. They are LGN (named after a repetitive amino acid sequence in the protein) (Mochizuki et al., 1996) and AGS3 (activator of G-protein signaling 3) (Blumer et al., 2002), which show 47.2 and 46.7% sequence identity with Pins, respectively, and 59.6% identity with each other. Mouse Pins has been shown to be a functional homolog of *Drosophila* Pins, and shows 92% homology with human LGN (Yu et al., 2003). LGN (677 amino acids) was first discovered in a yeast two-hybrid screen as a Gαi-binding protein (Mochizuki et al., 1996), whereas AGS3 (650 amino acids) was identified in a functional screen for receptor-independent activators of heterotrimeric G proteins (Takesono et al., 1999). LGN and AGS3 have similar domain architectures in which the amino-terminal third of the protein consists of seven tetratricopeptide repeats (TPR) followed by a linker region unique to each protein (Fig. 1A). At the carboxyl-terminal end of these proteins, there is a series of Gαi-Loco motifs also known as G-protein regulatory (GPR) motifs important in stabilizing the GDP-bound conformation of Gαi (Takesono et al., 1999; Cismowski et al., 2001; Knust, 2001; Blumer et al., 2002). The *Drosophila* protein Pins has the same protein domain architecture. Between the second and third TPR domains of LGN and Pins there is a protein motif with unknown function that is not found in AGS3 (Fig. 1B).

LGN is expressed in all rat tissues including neurons and glial cells whereas AGS3 is enriched primarily in CNS neurons (Blumer et al., 2002). Primary cultures of cortical neurons, astroglia, and microglia were all found to express LGN, but AGS3 is expressed primarily in neuronal cultures (Peterson et al., 2000; Blumer et al., 2002; Du et al., 2002). LGN and AGS3 have been shown to have distinct patterns of localization in primary neuronal cell cultures. In neural progenitor cells, they may play a role in spindle orientation as does Pins in *Drosophila* (Cai et al., 2003); however, whether they are localized asymmetrically or function as ACD determinants in human neural progenitor cells (hNPCs) is not known. In the developing postnatal brain, neurogenesis continues but whether this involves ACD of hNPCs has not been tested. Using postnatal, postmortem hNPC primary cultures, we have characterized the localization and dynamic distribution of LGN and AGS3 proteins in the mitotic divisions of this cell type.

MATERIALS AND METHODS

Human Subject Research Approval and Oversight

The hNPCs used in this study were obtained from postnatal postmortem patients (Schwartz et al., 2003) at the Children's Hospital of Orange County, with the approval and oversight of the hospital's Institutional Review Board. Informed consent for the donation of brain tissue was acquired before tissue acquisition, according to the protocol for the National Human Neural Stem Cell Resource (NHNSCR). Under the approval of the University of California Irvine Human Subjects Research Institutional Review Board, collected progenitor cell cultures were brought to the University of California, Irvine for analysis. All tissues were acquired and experiments conducted in compliance with NIH and institutional guidelines. For this study, cells grown from NHNSCR samples SC-23 and SC-27 were used.

Harvest and Collection of hNPCs

Human neural progenitor cell (hNPC) populations were collected, enriched, and cryopreserved at the Children's Hospital of Orange County NHNSCR (Schwartz et al., 2003) using methods adapted from previous studies (Vogel, 1992; Palmer et al., 1997, 1999, 2001).

Culture Media for hNPCs

The basal medium used was DMEM/F12, glutamine, and antibiotics (DGA) and contained Dulbecco's modified Eagle medium/F12 (DMEM/F12), high glucose (Irvine Scientific, Santa Ana, CA), glutamine, penicillin, streptomycin, amphotericin, gentamicin (Sigma, St. Louis, MO), and ciprofloxacin (Bayer, West Haven, CT). DGF medium containing DGA with 10% heat-inactivated fetal bovine serum (FBS; Hyclone, Logan, UT) was used for all washes and for glial cell culture.

Primary growth medium (PGM) consisted of DGF containing 10% BIT 9500 (Stem Cell Technologies), 40 ng/mL basic fibroblast growth factor (bFGF; Invitrogen, Carlsbad, CA), 20 ng/mL epidermal growth factor (EGF; Invitrogen), and 20 ng/mL platelet-derived growth factor-ab (PDGF-ab; Peprotech, Rocky Hill, NJ) as described previously (Palmer et al., 2001; Schwartz et al., 2003).

Growth medium (GM) was PGM without FBS as described previously (Palmer et al., 2001; Schwartz et al., 2003).

Differentiation medium (DM) was a 1:1 mixture of glial-conditioned-medium and DGA medium supplemented with 1% FBS, 100 nM all-*trans*-retinoic acid (Sigma), 20 ng/mL brain-derived neurotrophic factor (BDNF; Chemicon, Temecula, CA), and 20 ng/mL neurotrophin-3 (NT-3; Chemicon) as described previously (Palmer et al., 2001; Schwartz et al., 2003).

Enrichment for hNPCs

Cortical tissue was harvested from 25–26-week-old (estimated gestational age) premature infants. Tissues were chopped finely with scalpel blades and then incubated with mixing in DGA containing 2.5 U/mL papain (Worthington, Lakewood, NJ), 250 U/mL DNase I (Worthington), and 1 U/mL neutral protease (Roche, Indianapolis, IN). Partially digested tissues were dissociated further by centrifugation and trituration in three washes of DGF. Crude homogenates were plated initially onto fibronectin-coated plates in PGM. Plates had been treated previously with 200 μL/cm^2 of 5 μg/mL fibronectin overnight at 37°C; the fibronectin solution was then aspirated and the plates were allowed to air dry before introducing tissue homogenates. One-half of the medium was replaced daily with GM. Cell debris and nonadherent cells from the removed medium were pelleted by centrifugation and reintroduced into the culture with the fresh medium. After 10 days of culture, the plates were agitated by gentle tilting, all of the culture medium was removed, and 50% volume of fresh GM was added to the plates. The medium removed was centrifuged to pellet the cell debris and any nonadherent cells and 50% volume of the supernatant was put back into the plates. As each culture neared confluence it was lifted gently with collagenase and passaged into no more than twice the surface area from which it was lifted.

Immunocytochemistry

Immunocytochemistry was carried out as described previously (Dickinson-Anson et al., 1998). Cells were fixed for 10 min at room temperature in freshly prepared 4% formaldehyde (from paraformaldehyde) in phosphate-buffered saline (PBS), pH 7.45. The formaldehyde was removed and replaced with PBS containing 0.5% sodium azide and the plates were stored at 4°C until analyzed. Fixed cells were washed three times for 7 min in PBS, then incubated at room temperature for 1 hr with agitation in blocking buffer (0.15% Triton X-100, 0.05% Tween 20, and 5% serum from the host from which the secondary antibody was generated, in PBS). Cells were then rinsed in four changes of PBS over 5 min. Diluted primary antibody (1–10 μg/mL) was introduced in 3% serum and incubated either at room temperature for 1 hr or at 4°C overnight in a humidified chamber. The cells were then washed three times in PBS for 5 min. Cells were next incubated with dilute secondary antibody (1–5 μg/mL) in an opaque humidified chamber for 45 min at room temperature after which they were washed four times over 10 min. The slides were mounted with VectaShield mounting medium (Vector Laboratories, Burlingame, CA) and sealed.

Antibodies

Affinity-purified rabbit anti-LGN (Ser417-Lys449) peptide antibody directed toward the linker region of LGN and rabbit anti-LGN C-term peptide antibody (C, H) and rabbit anti-AGS3 described originally by Bernard et al. (2001) were provided generously by Drs. J. Blumer and S. Lanier (Department of Pharmacology, Louisiana State University Health Sciences Center). Mouse IgG anti-nestin, IgG anti-glial fibrillary acidic protein (anti-GFAP), and IgM anti-β-tubulin were purchased from BD Bioscience, (Palo Alto, CA). Mouse IgG anti-Gαi was obtained from Santa Cruz Biotechnology (Santa Cruz, CA). Affinity-purified anti-NuMA rabbit polyclonal antibody was kindly provided by Dr. D. Compton (Dartmouth Medical School, NH). Secondary antibodies used included: Alexa Fluor 488 goat anti-mouse and goat anti-rabbit, Alexa Fluor 568 goat anti-mouse and goat anti-rabbit, Alexa Fluor 647 goat anti-mouse and Alexa Fluor 568 and 647 goat anti-mouse IgM (Molecular Probes, Eugene, OR). TOPRO-3, propidium iodide (Molecular Probes) and DAPI (Sigma) were used as DNA stains.

Laser-Scanning Confocal Fluorescence Microscopy

Fixed hNPCs and live green fluorescent protein (GFP)-fusion protein-labeled hNPCs were prepared for indirect immunofluorescence and live imaging. They were observed using three different laser-scanning confocal microscopes and three different two-photon microscopes. The first microscope used was an MRC 1024 Bio-Rad/Nikon Diaphot 200 laser-scanning confocal microscope with *LaserSharp* image analysis software (Bio-Rad Microscience Division, Cambridge, MA). The second was a Leica inverted DMIRE2 microscope with a 400–850-nm spectral PMT detector. Laser sources for this microscope were: red (HeNe 633 nm/10 mW), orange (HeNe 594 nm/2 mW), green (HeNe 543 nm/1 mW), and blue (Ar 458 nm/5 mW; 488 nm/20 mW; 514 nm/20 mW). Images were collected and analyzed using the Leica Control Workstation. The third microscope was a Zeiss 510 Meta with an inverted Axiovert 200 microscope. This microscope used the following laser sources: Ar (458 nm; 477nm; 488 nm; 514nm; all at 30 mW) and HeNe (633 nm, 5 mW). The images collected using this system were analyzed using the Zeiss *LSM 3.0* software. For two-photon excitation on the Leica system, the MaiTai (Spectra-Physics) was used, and for the Zeiss system both the Chameleon (Coherent) and MaiTai were used. The Bio-Rad Radiance 2100 Multi-photon microscope was also used with the MaiTai laser. Images collected from this system were processed using *LaserSharp 2000* software (Bio-Rad Microscience Division).

Vectors and Transfection Methods

LGN-GFP fusion constructs of various LGN fragment lengths were made from pTRE-GFP-LGN-N (amino acids [AA] 1–341) or pGEXKG-LGN (full length), which were kindly provided by Dr. Q. Du (Department of Pharmacology, University of Virginia School of Medicine). LGN fragments were inserted N-terminal to and in frame with the GFP fragment of pEGFP (Clontech, Palo Alto, CA). In this way full-length, N-terminal and C-terminal LGN-GFP fusion constructs were generated. The GFP-AGS3 construct with AGS3 C-terminal to GFP was provided by Dr. S. Lanier. The gWiz constitutive GFP vector (Gene Therapy Systems, San Diego, CA) was used as a control for transfection and to observe the effect of constitutive GFP expression on the hNPCs.

Three transfection protocols were tested: Effectene (Qiagen, Valencia, CA), NeuroPorter (Gene Therapy Systems), and Lipofectamine (Invitrogen). The most efficient and best-tolerated transfection was achieved using a modified version of the cationic lipid-based NeuroPorter transfection system (Gene Therapy Systems). The NeuroPorter lipid was hydrated in GM according to the manufacturer's instructions, and then 8 μg of the vector was added to 110 μL of NeuroPorter solution. Before

transfection, each plasmid vector was purified using the QiAmp plasmid purification protocol (Qiagen, Valencia, CA). To ensure the plasmid was free of bacterial contaminants, the extracted plasmids were washed an additional three times before elution from the QiAmp purification column. The transfection mixture of DNA, hydrated NeuroPorter reagent and medium was incubated for 15 min and additional GM was introduced to give a volume of 5 mL, in a 60-mm culture dish or 500 μL in a single chamber of an eight-chambered slide. This final mix was added directly to the cells that had been grown to approximately 75% confluence. No evidence of cytotoxicity was seen 18 hr after the introduction of the transfection complex. The culture was retained in the mixture for an additional 6 hr, after which the mixture was removed and fresh GM was introduced. GFP-positive cells were observed 30 hr after transfection. Although these cells were transiently transfected and no antibiotic selection was used, in some cells expression persisted through 8 weeks after transfection, suggesting that stable transfection might have been achieved. After transfection, GFP-positive cells were either fixed for analysis by laser scanning confocal microscopy or were analyzed live using two-photon and standard fluorescent confocal time-lapse microscopy.

Colcemid Synchronization

To observe the effect of cell-cycle stage on the distribution of LGN and AGS3 in hNPCs, we introduced the M-phase blocker *N*-deacetyl-*N*-methylcolchicine (colcemid, 10 μg/mL). Cells were incubated with colcemid overnight and then fixed and immunocytochemically stained using the protocols outlined above.

Time-Lapse Microscopy

To study the dynamics of LGN and AGS3 distribution in live cells, we used constructs encoding LGN-GFP and AGS3-GFP transiently transfected into hNPCs grown to 75% confluence. Three different two-photon and fluorescent confocal microscopes were used to obtain time-lapse videomicrographs of these cells. A Nikon Eclipse TE300 inverted microscope equipped with a Photometrics Cool Snap Fx CCD camera (Roper Scientific), a Pro-Scan motorized inverted microscope stage (Prior Scientific) for multidimensional acquisition and a Lambda DG4 ultra high-speed wavelength switch (Sutter Instruments) for toggling between phase-contrast and fluorescent imaging was used. To maintain and image these cells successfully over a 24-hr period, environmental conditions, including temperature, humidity and CO_2 levels, were regulated carefully. The Nikon Eclipse TE300 microscope was enclosed in an opaque polyacrylate chamber. Temperature was maintained at 37°C using a heating system engineered by Dr. S.W. Rhee (Department of Biomedical Engineering, UCI). The two microscopes housed at Caltech were equipped with temperature regulation chambers. In all cases, medical grade 5% CO_2 balanced by air (AirGas) was bubbled through heated water and then passed into the culture dish via a small aperture in the top of a loose-fitting lid. In some instances, CO_2 levels were regulated by a Gilmont Instrument CO_2 sensor. The 492-nm GFP signal was detected using a variety of lasers in combination with the appropriate filter or detection device. Phase-contrast or differential interference contrast images were also collected. The exposure time of each pre-aligned laser was tested and set to avoid photobleaching and toxic effects. The hNPCs were imaged for periods approaching 24 hr. Data collected using this system were processed using *Metamorph v5.0r2* software (Universal Imaging Corp.) and Zeiss *LSM 3.0* software.

In collaboration with Dr. S. Fraser and the Caltech Biological Imaging Center, we examined the localization of LGN-GFP in live hNPCs using a Zeiss Pascal inverted laser-scanning microscope on an inverted Axiovert 200 microscope stand. Cells were also analyzed using a Zeiss 410 laser-scanning microscope on an inverted Zeiss Axiovert 135 microscope stand equipped with a motorized stage. GFP was excited at 488 nm using a continuous-wave argon ion laser. Images collected ranged from 512 × 512 to 2,042 × 2,048 pixels, with 12-bit (Pascal) or 8-bit (410) color depth.

GFP-positive transfected cells were imaged for 18–24 hr. DIC and fluorescent images were collected simultaneously every 5–15 min. Images were collected using 10–40× objectives and in some instances multiple positions within the same culture dish were studied in a single experiment.

RESULTS

LGN Localization in hNPCs

To determine the localization of LGN in hNPCs cultured under conditions favoring proliferation, cells were grown in growth medium (GM) for 1–2 weeks after passage, stained for immunofluorescence and counted. In 17% of these cells, LGN was restricted to one end of the cell (Fig. 2A–D) and in the remaining 83% LGN showed a fairly uniform cytoplasmic distribution. Similar results were obtained using each of the following microscopes: Figure 2A,B, Bio-Rad 1024; Figure 2C,E,F, Zeiss 510 Meta; and Figure 2D, Leica DMIRE2. A small fraction (~5%) (n = 54,560) of these cells exhibited small spots of LGN staining in the nucleus.

When the cells were grown in GM for 1–2 weeks, then transferred to DM for 3 weeks, LGN showed asymmetrical distribution at a lower frequency (~5%) but showed a focal staining pattern at a higher frequency (10–15%; Fig. 2E,F).

To examine LGN localization during mitosis, hNPCs were grown in GM and stained with anti-LGN and propidium iodide to label the DNA. Cells in interphase to early prophase showed uniform cytoplasmic distribution of the protein (Fig. 3A) but at late prophase (Fig. 3B), metaphase (Fig. 3C) and anaphase (Fig. 3D) LGN showed asymmetric localization. The percentage of cells showing asymmetric localization of LGN increased with progression through mitosis. In a count of adherent cells, 58% of cells in prophase (n = 31), 64% of cells in metaphase (n = 81), 92% of cells in anaphase (n = 39), and 100% of cells in telophase (n = 10) showed asymmetric LGN localization (Fig. 3E). LGN therefore becomes localized more asymmetrically during mitosis in these cells. We also noted several instances where LGN was localized asymmetrically in apparently non-mitotic cells, but these cells may have been in early prophase.

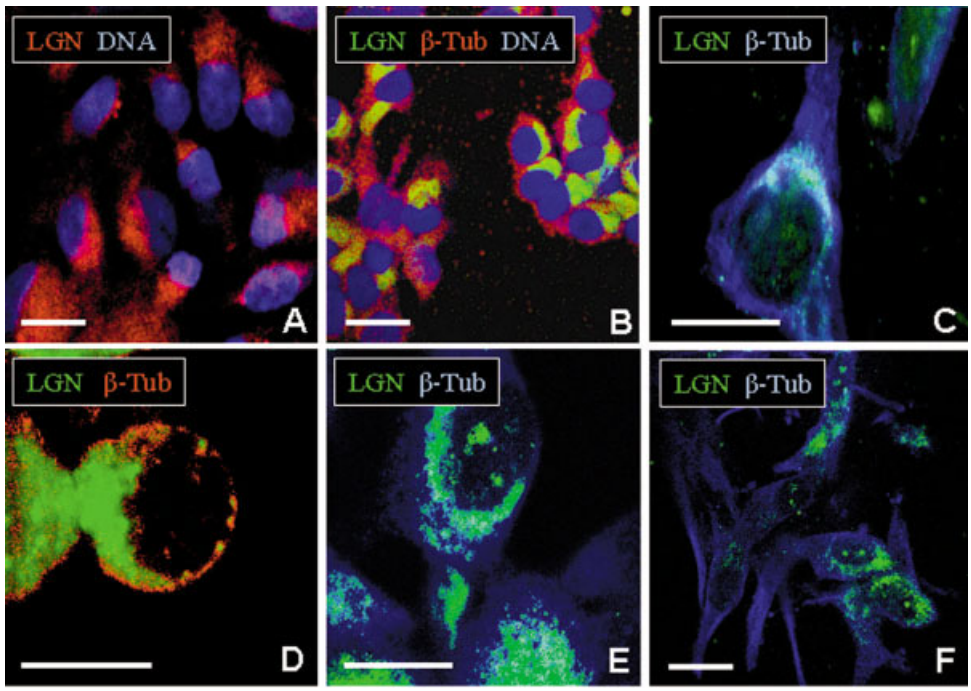

Fig. 2. LGN is localized asymmetrically in hNPCs. hNPCs were grown in growth medium (GM) or differentiation medium (DM), fixed, stained, and observed by laser-scanning confocal microscopy. **A:** GM-grown cells stained with anti-LGN (red) and TOPROIII/DNA (blue). **B:** GM-grown cells stained with anti-LGN (green), anti-β-tubulin (red) and TOPROIII/DNA (blue). **C:** GM-grown cells stained with anti-LGN (green) and anti-β-tubulin (blue). **D:** GM-grown cells stained with anti-LGN (green) and anti-β-tubulin (red). **E, F:** DM-grown cells stained with anti-LGN (green) and anti-β-tubulin (blue). Cells showing asymmetric localization of LGN are often found in clusters, whereas cells showing symmetric distribution are more often isolated. Scale bars = 10 μm.

In GM-grown cells, regions of LGN stain colocalized with regions staining for nestin, a marker used frequently to help identify neural progenitor cell populations (Fig. 4A) (Kappler et al., 1993; Kempermann et al., 2003). The LGN-positive region extended somewhat beyond the nestin-positive region. Nestin showed an asymmetric distribution in 54% of cells in late prophase to late anaphase (n = 108 mitotic cells).

AGS3 Localization in hNPCs

In GM-grown cells, AGS3 showed a diffuse cytoplasmic staining pattern, and did not show the same colocalization with nestin as did LGN (Fig. 4B). The diffuse distribution of AGS3 was maintained through interphase (Fig. 5A), prophase (Fig. 5B), metaphase (Fig. 5C) and anaphase (Fig. 5D).

LGN Localization in Colcemid-treated hNPCs

To explore further the relationship between cell-cycle stage and LGN distribution, hNPCs were treated with colcemid, which prevents microtubule polymerization (Oberlander et al., 1983) and traps the cells in metaphase (because AGS3 did not show any clear changes of expression or localization during the cell cycle, we did not include it in the colcemid study). Cells were grown in GM for 1–2 weeks after passage (Fig. 6A–C) or in GM for 1–2 weeks followed by DM for 3 weeks (Fig. 6D–F), then treated with colcemid (10 μg/mL) overnight. The cells were fixed, stained for fluorescence and observed by confocal microscopy using both single- and double-channel excitation. In GM-grown colcemid-treated cells, about 75% showed asymmetrical LGN localization, compared to 17% in untreated cells (Fig. 6G). This is consistent with the interpretation that the protein is distributed more asymmetrically at metaphase than at other cell-cycle stages. Colcemid treatment of DM-grown hNPCs, however, did not increase the percentage (~5%) of cells showing asymmetric localization of LGN.

In hNPCs grown in GM and treated with colcemid, LGN showed asymmetric cytoplasmic localization and strong colocalization with nestin (Fig. 6A–C). LGN staining extended somewhat beyond the regions positive for nestin as in the untreated cells. As mentioned earlier, ~5% of these cells exhibited single or double nuclear foci of LGN stain. In cells transferred to DM before colcemid treatment and fixation, however, the number showing single or double nuclear foci of LGN staining increased to 86% (n = 34,012) (Fig. 6E,F) whereas nestin distribution (Fig. 6D,F) remained similar to that seen in GM. The double foci were similar to those observed using anti-NuMA antibody (Fig. 7A–D), consistent with previous studies that link LGN with NuMA activity during mitosis in differentiated cell types (Du et al., 2002). We observed

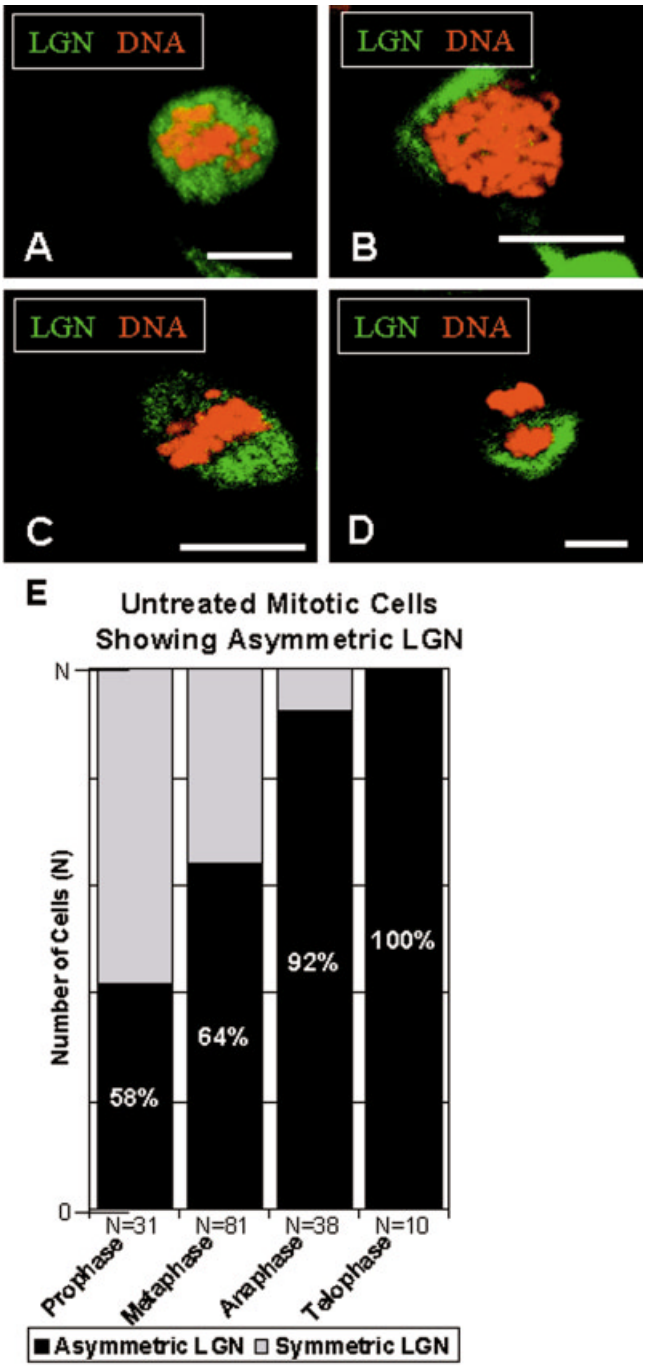

Fig. 3. LGN is localized asymmetrically in hNPCs during mitosis and the percentage of cells showing asymmetric LGN localization increases with mitotic progression. hNPCs grown in GM and stained with anti-LGN (green) and propidium iodide/DNA (red) during interphase (**A**), prophase (**B**), metaphase (**C**), and anaphase (**D**). Scale bars = 10 μm. **E:** Count of cells showing asymmetric localization of LGN at various mitotic stages.

localization to the midbody structure between dividing cells, as has been reported for PC12 and COS7 cells (Blumer et al., 2002), only in rare cases of DM-grown cells.

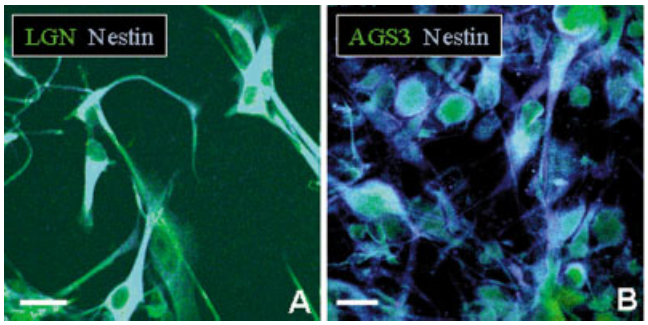

Fig. 4. LGN and AGS3 show different patterns of localization in GM-grown hNPCs. Confocal images of hNPCs stained with anti-LGN (green) and anti-nestin (blue) (**A**), or anti-AGS3 (green) and anti-nestin (blue) (**B**). Scale bars = 10 μm.

Time-Lapse Microscopy of GFP-labeled LGN and AGS3

The asymmetric segregation of LGN during mitosis of hNPCs was confirmed using time-lapse video microscopy. Vectors encoding LGN-GFP and AGS3-GFP fusion proteins were transfected into hNPCs, and the live cells were observed over 24 hr using confocal microscopy (Fig. 8). Four separate instances of mitotic divisions were captured in this study, and in all cases the LGN-GFP signal segregated into only one of the two daughter cells (Figs. 8, Supplemental Fig. 1, Supplemental Time-Lapse 1,2).

Although we found cells expressing LGN and dividing asymmetrically (Fig. 8), many of the cells strongly expressing LGN-GFP seemed to undergo abortive mitosis, and LGN was not localized asymmetrically in these cells (Supplemental Fig. 2, Supplemental Time-Lapse 3). After elongating like dividing cells, the cells retracted to their original shape without dividing. This phenomenon has been reported previously in MDCK cells transiently expressing Myc-LGN-N, and interpreted as showing that overexpression of LGN inhibits the stabilization of microtubules, preventing mitotic progression (Du et al., 2002). The labeled cells that did complete division showed a weaker GFP signal than did those undergoing abortive division, suggesting that they were expressing the construct at a lower level and were thus able to proceed through mitosis. Instances of LGN-GFP induction were also recorded (Supplemental Fig. 3, Supplemental Time-Lapse 4) wherein hNPCs began to show expression of LGN-GFP during the course of the time-lapse imaging. We also observed cells in which the signal declined during the study, but these cells died shortly afterwards, suggesting that the declining signal was associated with apoptosis rather than downregulation of LGN expression.

During a 24-hr observation period we observed no mitotic AGS3-GFP-positive cells although these cells did display some morphologic changes (Supplemental Fig. 4, Supplemental Time-Lapse 5). Unlike LGN-GFP-positive cells, abortive mitosis was not observed in AGS3-GFP-positive hNPCs. Human NPCs transfected with gWiz-GFP (Gene Therapy Systems), a control GFP vector en-

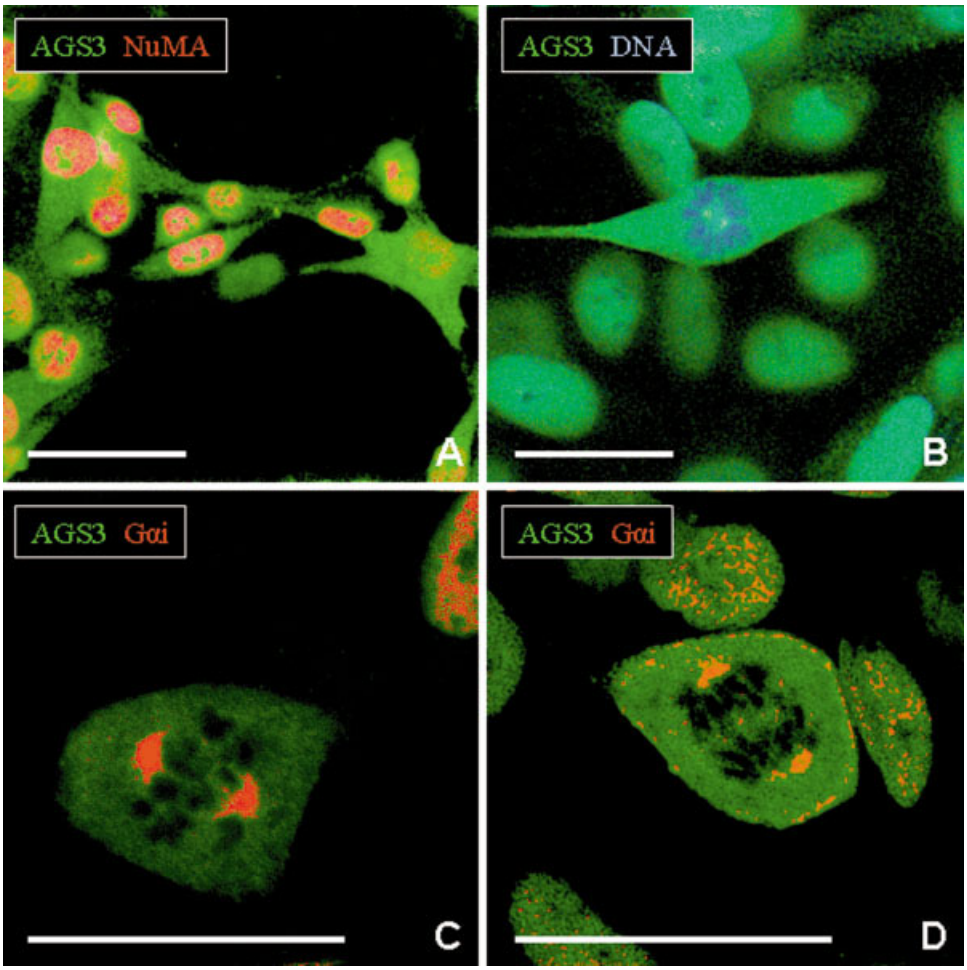

Fig. 5. AGS3 is distributed symmetrically in mitotic hNPCs. hNPCs grown in GM stained with anti-AGS3 (green), anti-NuMA (red) and/or TOPROIII/DNA (blue) during interphase (**A**), prophase (**B**), metaphase (**C**), and anaphase (**D**). Scale bars = 10 μm.

coding GFP under the CMV promoter, as a control divided apparently normally, so GFP itself does not seem to affect mitosis in these cells.

DISCUSSION

Our results show that the two human homologs of *Drosophila* Pins, LGN and AGS3, are localized differently in primary cultures of hNPCs from postnatal, postmortem brains. In these cells LGN, like *Drosophila* Pins, is distributed asymmetrically in a cell cycle-dependent manner and segregates to one of the two daughter cells of the division, but AGS3 shows a more diffuse cytoplasmic localization without asymmetry. As with Pins, the subcellular localization of LGN in non-differentiating hNPCs is related to cell cycle stage. In cells undergoing mitosis, LGN segregates to one side of the dividing cell and into one of the daughters, but during interphase the protein seems localized uniformly throughout the cytoplasm. The data suggest that hNPCs undergo ACD and that LGN may act as an ACD determinant during these divisions.

In untransfected hNPCs stained with anti-LGN antibodies, LGN was localized asymmetrically as is Pins, but in cells expressing the LGN-GFP protein, the fluorescently tagged LGN accumulated in the cytoplasm. Because the LGN-GFP protein expressed in transfected hNPCs was under the control of the constitutive CMV promoter, more LGN-GFP may have been produced in these cells than could be localized in the normal pattern.

In hNPCs grown in DM, LGN localizes in single or double nuclear foci that seem to correspond to regions of the spindle poles, as shown previously in non-progenitor cell cultures (Blumer et al., 2002) where LGN acts as a negative regulator of aster formation and is known to bind to the mitotic protein NuMA (Du et al., 2001, 2002). NuMA induces bundling and stabilization of microtubules (Compton et al., 1991; Zeng et al., 1994a; He et al., 1995; DeChiara et al., 1996; Haren and Merdes, 2002), suggesting that LGN may also function transiently in regulation of the mitotic spindle, as described in other non-progenitor

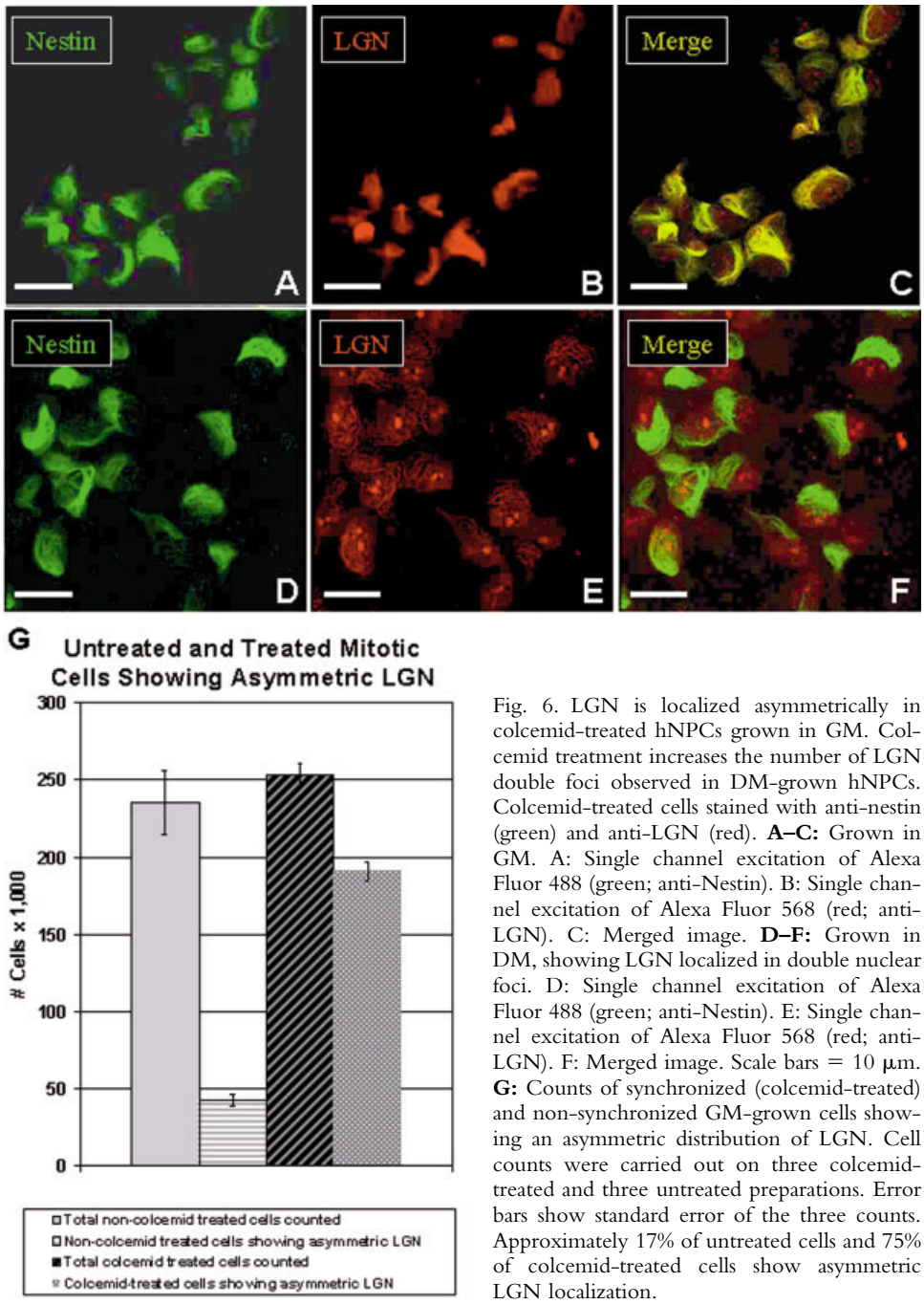

Fig. 6. LGN is localized asymmetrically in colcemid-treated hNPCs grown in GM. Colcemid treatment increases the number of LGN double foci observed in DM-grown hNPCs. Colcemid-treated cells stained with anti-nestin (green) and anti-LGN (red). **A–C:** Grown in GM. A: Single channel excitation of Alexa Fluor 488 (green; anti-Nestin). B: Single channel excitation of Alexa Fluor 568 (red; anti-LGN). C: Merged image. **D–F:** Grown in DM, showing LGN localized in double nuclear foci. D: Single channel excitation of Alexa Fluor 488 (green; anti-Nestin). E: Single channel excitation of Alexa Fluor 568 (red; anti-LGN). F: Merged image. Scale bars = 10 μm. **G:** Counts of synchronized (colcemid-treated) and non-synchronized GM-grown cells showing an asymmetric distribution of LGN. Cell counts were carried out on three colcemid-treated and three untreated preparations. Error bars show standard error of the three counts. Approximately 17% of untreated cells and 75% of colcemid-treated cells show asymmetric LGN localization.

cell cultures (Compton and Cleveland, 1994; Zeng et al., 1994b; Doe, 1996; Du et al., 2001, 2002). LGN has been shown previously to bind to NuMA and affect the polymerization of microtubules (Du et al., 2001). This function could be responsible for the apparent disruption of mitosis caused by overexpression of GFP-tagged LGN.

Our results show asymmetric localization of nestin in colcemid-treated hNPCs grown in GM. Nestin is an intermediate filament protein that is expressed predominantly in progenitor cells of the CNS (Dahlstrand et al., 1995) and upon terminal neural differentiation is downregulated and replaced by neurofilaments (Hockfield and McKay, 1985). It has been used as a marker for progenitor cells (Hockfield and McKay, 1985) but has not been observed previously to show asymmetric localization. Nestin and LGN showed clear subcellular colocalization in metaphase-trapped, colcemid-treated hNPCs, suggesting that these two proteins may interact with each other in a manner regulated by the cell cycle. Because nestin is a microfilament protein, LGN may also affect microfilament

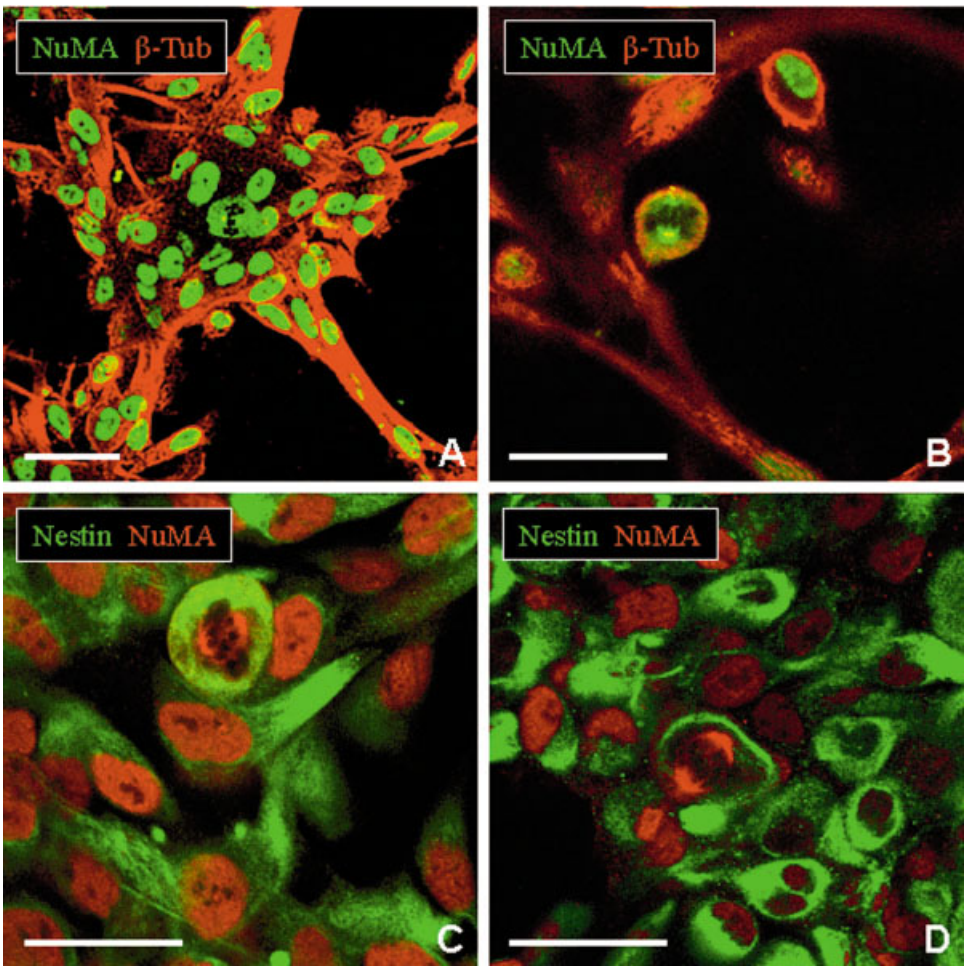

Fig. 7. NuMA also shows a double focus pattern in mitotic hNPCs. **A:** Aggregate of hNPCs grown in GM stained with anti-β-tubulin (red) and anti-NuMA (green). Note the mitotic cell in the center of the neurosphere showing double foci of NuMA at the spindle poles of the mitotic cell (metaphase chromosomes exclude stain and appear black). **B:** Adherent hNPCs stained as in (A) showing similar localization of NuMA and β-tubulin, **C, D:** Adherent hNPCs stained with anti-NuMA (red) and anti-nestin (green). Scale bars = 10 μm.

protein distribution and polarization during the cell cycle or, conversely, nestin may affect LGN localization. Although the exact role of nestin in ACD remains to be established, this is the first evidence suggesting that nestin may play a role in the process.

AGS3, a second human homolog of the *Drosophila* protein Pins, is expressed diffusely in actively dividing hNPCs grown in GM and DM. Its expression seems to be increased during differentiation, but unlike LGN it does not show asymmetry or any obvious change related to cell cycle progression. AGS3 also differs from LGN in that it is restricted to neurons and is not found in glial cells (Blumer et al., 2002). AGS3, therefore, may play a role in later differentiating divisions of neuronal precursors or neuroblasts rather than in ACD of hNPCs. LGN and AGS3 are both expressed in rat neuronal cell cultures with differing patterns of subcellular localization (LGN localizes to the nucleus but AGS3 does not), but no functional studies have been reported for these cells (Blumer et al., 2002).

It is not clear what characteristics of the amino acid sequences of LGN and AGS3 determine their different subcellular localizations. One possibility is the PFAM domain present in LGN and Pins but absent from AGS3 (Fig. 1A). Another possibility is the third TPR repeat of ASG3 (Fig. 1B), which is so divergent from the corresponding region in the other two proteins that it is not recognized as a TPR repeat by the SMART domain analysis program (http://smart.embl.heidelberg.de). Site-directed mutagenesis of these regions could determine the one responsible for the different behavior of Pins/LGN versus AGS3.

Additional proteins are known to play a role in ACD of *Drosophila* neuroblasts (Knoblich, 2001). Many of these proteins have clear human sequence homologs, but it remains to be determined whether the homologs have

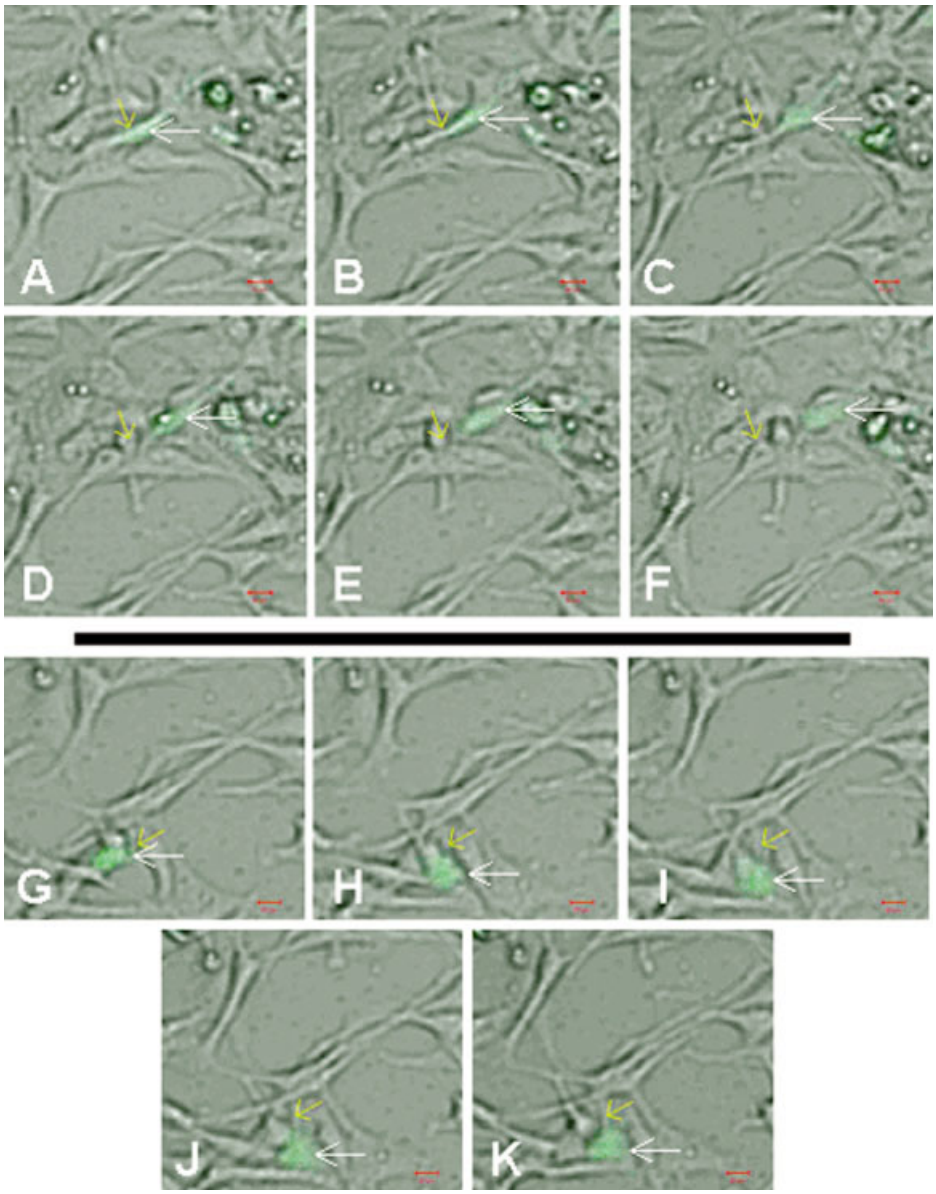

Fig. 8. GFP-LGN is localized asymmetrically in live mitotic hNPCs. Time-lapse videomicrographs of hNPCs in GM transfected with GFP-labeled LGN (green), showing two examples (**A–F** and **G–K**) of ACD. A: 960 min. B: 965 min. C: 970 min. D: 975 min. E: 980 min. F: 985 min. G: 160 min. H: 165 min. I: 170 min. J: 175 min. K: 180 min. Arrows show ACD; white; GFP^+ daughter cell; yellow, GFP^- daughter cell.

similar functions. Human NPC cultures provide an excellent system for determining the functions of these elements.

ACKNOWLEDGMENTS

This research was supported in part by grants from the NCI (grant CA91043 to P.J.B.), the Salk Institute for Biological Studies (to P.H.S.), the CHOC Foundation for Children (to P.H.S.), the United Mitochondrial Disease Foundation (to P.H.S.), and the National Institute of Child Health and Human Development (training grant HD07029 to T.F.). We thank Drs. S. Fraser and M. Dickinson of the Biological Imaging Center, California Institute of Technology, Pasadena, for their technical assistance and advice on confocal and two-photon microscopy and for use of their facilities. We thank Drs. J. Blumer and S. Lanier (Department of Pharmacology, Louisiana State University Health Sciences Center), Dr. Q. Du (Department of Pharmacology, University of Virginia School of Medicine), Dr. D. Compton (Dartmouth Med-

ical School, New Hampshire), and Dr. S.W. Rhee (Department of Biomedical Engineering, UCI) for the gifts of reagents. We also thank D. Fuja for plasmid construction and confocal imaging.

REFERENCES

Bellaiche Y, Radovic A, Woods DF, Hough CD, Parmentier ML, O'Kane CJ, Bryant PJ, Schweisguth F. 2001. The Partner of Inscuteable/Discs-large complex is required to establish planar polarity during asymmetric cell division in *Drosophila*. Cell 106:355–366.

Bernard ML, Peterson YK, Chung P, Jourdan J, Lanier SM. 2001. Selective interaction of AGS3 with G-proteins and the influence of AGS3 on the activation state of G-proteins. J Biol Chem 276:1585–1593.

Blumer JB, Chandler LJ, Lanier SM. 2002. Expression analysis and subcellular distribution of the two G-protein regulators AGS3 and LGN indicate distinct functionality. Localization of LGN to the midbody during cytokinesis. J Biol Chem 277:15897–15903.

Bulgheresi S, Kleiner E, Knoblich JA. 2001. Inscuteable-dependent apical localization of the microtubule-binding protein Cornetto suggests a role in asymmetric cell division. J Cell Sci 114:3655–3662.

Cai Y, Yu F, Lin S, Chia W, Yang X. 2003. Apical complex genes control mitotic spindle geometry and relative size of daughter cells in *Drosophila* neuroblast and pI asymmetric divisions. Cell 112:51–62.

Ceron J, Gonzalez C, Tejedor FJ. 2001. Patterns of cell division and expression of asymmetric cell fate determinants in postembryonic neuroblast lineages of *Drosophila*. Dev Biol 230:125–138.

Cismowski MJ, Takesono A, Bernard ML, Duzic E, Lanier SM. 2001. Receptor-independent activators of heterotrimeric G-proteins. Life Sci 68:2301–2308.

Clarke DL, Johansson CB, Wilbertz J, Veress B, Nilsson E, Karlstrom H, Lendahl U, Frisen J. 2000. Generalized potential of adult neural stem cells. Science 288:1660–1663.

Compton DA, Cleveland DW. 1994. NuMA, a nuclear protein involved in mitosis and nuclear reformation. Curr Opin Cell Biol 6:343–346.

Compton DA, Yen TJ, Cleveland DW. 1991. Identification of novel centromere/kinetochore-associated proteins using monoclonal antibodies generated against human mitotic chromosome scaffolds. J Cell Biol 112: 1083–1097.

Dahlstrand J, Lardelli M, Lendahl U. 1995. Nestin mRNA expression correlates with the central nervous system progenitor cell state in many, but not all, regions of developing central nervous system. Brain Res Dev Brain Res 84:109–129.

DeChiara TM, Bowen DC, Valenzuela DM, Simmons MV, Poueymirou WT, Thomas S, Kinetz E, Compton DL, Rojas E, Park JS, Smith C, DiStefano PS, Glass DJ, Burden SJ, Yancopoulos GD. 1996. The receptor tyrosine kinase MuSK is required for neuromuscular junction formation in vivo. Cell 85:501–512.

Dickinson-Anson H, Aubert I, Gage FH, Fisher LJ. 1998. Hippocampal grafts of acetylcholine-producing cells are sufficient to improve behavioural performance following a unilateral fimbria-fornix lesion. Neuroscience 84:771–781.

Doe CQ. 1996. Spindle orientation and asymmetric localization in *Drosophila*: both inscuteable? Cell 86:695–697.

Du Q, Stukenberg PT, Macara IG. 2001. A mammalian Partner of inscuteable binds NuMA and regulates mitotic spindle organization. Nat Cell Biol 3:1069–1075.

Du Q, Taylor L, Compton DA, Macara IG. 2002. LGN blocks the ability of NuMA to bind and stabilize microtubules. A mechanism for mitotic spindle assembly regulation. Curr Biol 12:1928–1933.

Haren L, Merdes A. 2002. Direct binding of NuMA to tubulin is mediated by a novel sequence motif in the tail domain that bundles and stabilizes microtubules. J Cell Sci 115:1815–1824.

He D, Zeng C, Brinkley BR. 1995. Nuclear matrix proteins as structural and functional components of the mitotic apparatus. Int Rev Cytol 162:1–74.

Hockfield S, McKay RD. 1985. Identification of major cell classes in the developing mammalian nervous system. J Neurosci 5:3310–3328.

Jiang Y, Jahagirdar BN, Reinhardt RL, Schwartz RE, Keene CD, Ortiz-Gonzalez XR, Reyes M, Lenvik T, Lund T, Blackstad M, Du J, Aldrich S, Lisberg A, Low WC, Largaespada DA, Verfaillie CM. 2002. Pluripotency of mesenchymal stem cells derived from adult marrow. Nature 418:41–49.

Kappler C, Meister M, Lagueux M, Gateff E, Hoffmann JA, Reichhart JM. 1993. Insect immunity. Two 17 bp repeats nesting a kappa B-related sequence confer inducibility to the diptericin gene and bind a polypeptide in bacteria-challenged *Drosophila*. EMBO J 12:1561–1568.

Kempermann G, Gast D, Kronenberg G, Yamaguchi M, Gage FH. 2003. Early determination and long-term persistence of adult-generated new neurons in the hippocampus of mice. Development 130:391–399.

Knoblich JA. 2001. Asymmetric cell division during animal development. Nat Rev Mol Cell Biol 2:11–20.

Knust E. 2001. G protein signaling and asymmetric cell division. Cell 107:125–128.

Matsuzaki F. 2000. Asymmetric division of *Drosophila* neural stem cells: a basis for neural diversity. Curr Opin Neurobiol 10:38–44.

Mochizuki N, Cho G, Wen B, Insel PA. 1996. Identification and cDNA cloning of a novel human mosaic protein, LGN, based on interaction with G alpha i2. Gene 181:39–43.

Oberlander H, Lynn DE, Leach CE. 1983. Inhibition of cuticle production in imaginal discs of *Plodia interpunctella* cultured in vitro: effects of Colcemid and Vinblastine. J Insect Physiol 29:47–53.

Palmer TD, Markakis EA, Willhoite AR, Safar F, Gage FH. 1999. Fibroblast growth factor–2 activates a latent neurogenic program in neural stem cells from diverse regions of the adult CNS. J Neurosci 19:8487–8497.

Palmer TD, Schwartz PH, Taupin P, Kaspar B, Stein SA, Gage FH. 2001. Cell culture. Progenitor cells from human brain after death. Nature 411:42–43.

Palmer TD, Takahashi J, Gage FH. 1997. The adult rat hippocampus contains primordial neural stem cells. Mol Cell Neurosci 8:389–404.

Parmentier ML, Woods D, Greig S, Phan PG, Radovic A, Bryant P, O'Kane CJ. 2000. Rapsynoid/Partner of inscuteable controls asymmetric division of larval neuroblasts in *Drosophila*. J Neurosci 20:RC8.

Peterson YK, Bernard ML, Ma H, Hazard S, III, Graber SG, Lanier SM. 2000. Stabilization of the GDP-bound conformation of Gialpha by a peptide derived from the G-protein regulatory motif of AGS3. J Biol Chem 275:33193–33196.

Potten CS. 1997. Stem cells. London, San Diego: Academic Press.

Rathjen J, Haines BP, Hudson KM, Nesci A, Dunn S, Rathjen PD. 2002. Directed differentiation of pluripotent cells to neural lineages: homogeneous formation and differentiation of a neurectoderm population. Develop 129:2649–2661.

Schaefer M, Knoblich JA. 2001. Protein localization during asymmetric cell division. Exp Cell Res 271:66–74.

Schaefer M, Shevchenko A, Knoblich JA. 2000. A protein complex containing Inscuteable and the Galpha-binding protein Pins orients asymmetric cell divisions in *Drosophila*. Curr Biol 10:353–362.

Schwartz PH, Bryant PJ, Fuja TJ, Su H, O'Dowd DK, Klassen HJ. 2003. Isolation and characterization of neural progenitor cells from post-mortem human cortex. J Neurosci Res 74:838–851.

Schwartz RE, Reyes M, Koodie L, Jiang Y, Blackstad M, Lund T, Lenvik T, Johnson S, Hu WS, Verfaillie CM. 2002. Multipotent adult progenitor cells from bone marrow differentiate into functional hepatocyte-like cells. J Clin Invest 109:1291–1302.

Spana EP, Kopczynski C, Goodman CS, Doe CQ. 1995. Asymmetric localization of numb autonomously determines sibling neuron identity in the *Drosophila* CNS. Development 121:3489–3494.

Takesono A, Cismowski MJ, Ribas C, Bernard M, Chung P, Hazard S, III, Duzic E, Lanier SM. 1999. Receptor-independent activators of heterotrimeric G-protein signaling pathways. J Biol Chem 274:33202–33205.

Temple S. 2001. Stem cell plasticity—building the brain of our dreams. Nat Rev Neurosci 2:513–520.

Vogel EW. 1992. Tests for recombinagens in somatic cells of *Drosophila*. Mutat Res 284:159–175.

Yu F, Morin X, Cai Y, Yang X, Chia W. 2000. Analysis of partner of inscuteable, a novel player of *Drosophila* asymmetric divisions, reveals two distinct steps in inscuteable apical localization. Cell 100:399–409.

Yu F, Morin X, Kaushik R, Bahri S, Yang X, Chia W. 2003. A mouse homologue of *Drosophila* pins can asymmetrically localize and substitute for pins function in *Drosophila* neuroblasts. J Cell Sci 116:887–896.

Zeng C, He D, Berget SM, Brinkley BR. 1994a. Nuclear-mitotic apparatus protein: a structural protein interface between the nucleoskeleton and RNA splicing. Proc Natl Acad Sci USA 91:1505–1509.

Zeng C, He D, Brinkley BR. 1994b. Localization of NuMA protein isoforms in the nuclear matrix of mammalian cells. Cell Motil Cytoskeleton 29:167–176.